PRELIMINARY STUDY ON THE TRANSLUNAR HALO ORBITS OF THE REAL EARTH-MOON SYSTEM

M.A. ANDREU
Dept. Matemàtica Aplicada i Anàlisi, Univ. Barcelona,
Gran Via 585, 08007 Barcelona, Spain.
e-mail: mangel@maia.ub.es

Abstract. The computation of translunar Halo orbits of the real Earth-Moon system (REMS) has been an open problem for a long time, but now, it is possible to compute Halo orbits of the REMS in a systematic way. In this paper, we describe the method used for the numerical computation of Halo orbits for a time span longer than 41 years. Halo orbits of the REMS are computed from quasi-periodic Halo orbits of the Quasi-bicircular Problem (QBCP). The QBCP is a model for the dynamics of a spacecraft in the Earth-Moon-Sun system. It is a Hamiltonian system with three degrees of freedom and depending periodically on time. In this model, Earth, Moon and Sun are moving in a self-consistent motion close to bicircular. The computed Halo orbits of the REMS are compared with the family of Halo orbits of the QBCP. The results show that the QBCP is a good model to understand the main features of the Halo family of the REMS.

Keywords: Halo orbits, Earth-Moon system, quasi-bicircular problem, invariant tori.

1. Introduction

In the last years, an increase of the application of dynamical systems techniques in the design of trajectories in astrodynamics has been observed. The knowledge of the dynamics of a problem helps to get optimal transfer trajectories and design control orbits strategies, which probably would not be obtained from a single numerical approach. Moreover, the dynamical systems approach provides more insight of the problem studied and it can offer families of solutions depending on one or more parameters. This fact gives the possibility of a more flexible mission design and it allows to prepare the contingency planning of a space mission.

Stable and unstable manifolds of periodic and quasi-periodic orbits are common objects in the Dynamical Systems world, which have a lot of applications in Astrodynamics. The stable manifold of a Halo orbit can be used to transfer a spacecraft from the vicinity of the Earth to a Halo orbit around L_1 of the Earth-Sun system (Gómez et al., 1993). Intersections of stable and unstable manifolds of different dynamical objects are called a heteroclinic connections. They allow

to perform transfers from different regions of the phase space with a theoretical zero cost transfer. For instance, in the RTBP frame, there are heteroclinic connections between orbits around L_1 and L_2 (Gómez et al., 2000) (Koon et al., 2000). Invariant manifolds are also used in the design of control strategies. When a spacecraft is deviating from a nominal orbit, instead of looking for a manoeuvre to return it to the nominal path, it is only necessary to look for a manoeuvre to insert the spacecraft in the stable manifold of the nominal orbit, and there the dynamics will carry it up to the desired orbit (Gómez et al., 1998).

Moreover, a global knowledge of the dynamics of a problem can provide new available trajectories of a spacecraft. These new possibilities can direct you to a new design for new space missions, which never would be dreamt of without the mentioned knowledge of the dynamics. An example of that, is the TPF mission (Terrestrial Planet Finder), which is planning to use an infrared interferometer with a baseline of about 100 m. For such purpose, the TPF mission is going to use a constellation of five spacecrafts flying in formation in the vicinity of a Halo orbit around the L_2 libration point of the Earth-Sun system. The possibility of a flight formation near a Halo orbit is fairly understood from the dynamics in the center manifold around the L_2 point of the RTBP (Gómez et al., 2001) (Gómez et al., 1998) (Jorba et al., 1999).

On the other hand, in the last years, the beginning of utilisation of four-body problems as models of reference for the design of some space missions has also been seen. The Genesis mission, launched in August 2001, will be in a Halo orbit around L_1 of the Earth-Sun system for two years with the purpose of collecting solar wind samples (Koon et al., 1999). After that, the spacecraft will come back to the Earth, but it should enter in the Earth's atmosphere during daylight time, because the capsule would be caught by helicopters before it lands. A return orbit without deterministic manoeuvres is possible by using an orbit passing within the vicinity of the L_2 point of the Earth-Sun system. It has been seen that the Moon also plays an important role in the existence of such return orbit. For the computation of the nominal orbit, the Bicircular Problem (BCP) has been used. The BCP is a four body problem which considers the Earth and the Moon moving in circular orbits around their barycenter, and the barycenter moving also in a circular orbit around the Sun. The BCP was introduced by (Huang, 1960) and it has been used especially to study the motion near the triangular libration points of the Earth-Moon system (Wiesel, 1984) (Gómez et al., 1987) (Jorba, 1999).

Another space mission using a complex dynamical trajectory is the "Petit Grand Tour". This mission is scheduled to visit several moons of Jupiter. The trajectory is designed based on the fact that it is pos-

sible to find paths passing within the neighbourhood of several moons and being ballistically captured by each moon for a prescribed time interval (Gómez et al., 2001). To model the dynamics of a spacecraft going from a moon to another one, say for instance, Ganymede and Europa, a bicircular problem (Jupiter-Ganymede-Europa-spacecraft) is used. The desired trajectory is obtained by considering the heteroclinic connections between the manifolds of the L_1 and L_2 points of the Jupiter-Ganymede system and the corresponding ones of the Jupiter-Europa system. In this case, it has been shown that the transfer ΔV needed is about a half of the one needed using a classical Hohmann transfer.

In 1993, Belbruno and Miller discovered the existence of orbits which allow to travel from the Earth to the Moon using only 80% of the fuel of a classical Hohmann transfer (Belbruno et al., 1993). However, the flight time increases from 5 days of the classical transfer to 5 months for the Belbruno's trajectories. Nevertheless, Belbruno's trajectories can be useful on robotic missions with the goal of sending heavy machinery from the Earth to the Moon. The existence of Belbruno's transfer can not be understood in the RTBP frame. It is necessary to use a four body model Earth-Moon-Sun-spacecraft and study the connections between the manifolds of L_1 and L_2 of the Earth-Moon system with the manifolds of L_1 and L_2 of the Earth-Sun system (Koon et al., 2001)

Despite the BCP has been widely used, it is not a self-consistent model because the motion of primaries is not a solution of the Three Body Problem. The existence of the Sun modifies the Earth-Moon distance and so it can not be constant (Szebehely, 1967). The Quasi-bicircular problem (QBCP) is a model similar to BCP but it is self-consistent. The QBCP was introduced by the author in (Andreu, 1998). We want to emphasise that the use of the QBCP, instead of the BCP, does not introduce any increase of the complexity of the problem. Both models are Hamiltonian systems with three degrees of freedom, which depend periodically on time. The lack of consistency of the BCP is especially relevant in the vicinity of the libration points of the Earth-Moon system. In these zones, important dynamical discrepancies can be found between the BCP and QBCP (see chapter 2 of (Andreu, 1998)).

The motivation to introduce the QBCP was the interest of the knowledge of the dynamics in the neighbourhood of the L_2 of the real Earth-Moon system (REMS). The most accurate available model is considered as REMS and it comes from the JPL ephemeris.

In 1970, Farquhar proposed the use of translunar Halo orbits as a means to establish a continuous communication link between the Earth and the far side of the Moon (Farquhar, 1970). However, it was difficult to find Halo-like orbits of the REMS for a long time span. The main

difficulty came from the fact that the RTBP was not a sufficiently good model of the dynamics of a spacecraft in the vicinity of the Earth-Moon libration points. The influence of the Sun is not negligible because it highly perturbs the orbit of the Moon. The discrepancies between the orbit of the Moon and a Keplerian approximation orbit are known from ancient time. We recommend (Gutzwiller, 1998) for a nice exposition about the history of the Lunar theory.

In spite of the fact the motion of the Moon is very complicated and the QBCP depends only on one frequency, the QBCP has been shown to be useful to understand the main features of the dynamics of a spacecraft in the zone of the L_2 libration point of the REMS. For this purpose, some other more accurate analytical models can be used. However, the QBCP is a model sufficiently simple to be studied and sufficiently complex to keep the main features of the REMS.

A brief introduction to the QBCP is given in section 2. The QBCP is a restricted four body problem where the three primaries are revolving in a quasi-bicircular motion. The QBCP is a Hamiltonian system with three degrees of freedom and depends periodically on time. The corresponding frequency is the synodic frequency of the Moon.

Section 3 explains the Jorba's method for the computation of an invariant torus in a dynamical system. This method is used for the computation of Halo orbits of the QBCP, which are two-dimensional (2D) invariant tori. This method can be combined with a continuation method in order to follow a family of tori depending on one parameter.

Section 4 deals with the description of the family of Halo orbits of the QBCP, which is a Cantorian set of 2D tori. Nevertheless, several branches of the family can be computed as if they were a continuous. The main feature of the Halo family is the existence of the 1:2 resonance between the synodic period of the Moon and the inner period of the Halo orbits. The study of the Halo family also reveals the existence of some big gaps, which might be related to resonances with the normal frequency.

Section 5 is devoted to the numerical computation of Halo orbits of the REMS. The method used for this computation is a relaxed Newton's method. A parallel shooting technique is also included in the algorithm due to the fact that Halo orbits are highly unstable. Halo orbits of the QBCP are used as an initial guess for the Newton's method.

In this section, the computed Halo orbits are compared with the Halo family of the QBCP. It is shown that there is a nice agreement between both families of Halo orbits. The agreement gives a clear evidence of the usefulness of the QBCP as a model of reference to study the Halo orbits of the REMS.

The analysis of the frequencies of the computed orbits show what frequencies of the motion of the Moon are important to understand the main features of the Halo family. Apart from the synodic frequency, it is shown that the anomalistic frequency also plays an important role. Another frequency of the Moon which also arises from the Fourier analysis is the difference between the anomalistic and the draconitic frequencies. Other frequencies of the motion of the Moon are shown to be rather less important.

2. The Quasi-bicircular Problem

The Quasi-bicircular problem (QBCP) is a restricted four body problem where three masses are revolving in a quasi-bicircular motion, the fourth mass being small and not influencing the motion of the primaries. The QBCP for the mass parameters of the Earth–Moon–Sun was introduced by the author in (Andreu, 1998). Let B_{em} be the center of mass of the Earth–Moon system and B the one of the full system. In the QBCP, the motion of the Earth, Moon and Sun is a solution close to bicircular of the general Three Body Problem. This means that the Earth and Moon around B_{em}, and Sun and B_{em} around B, are moving close to circular orbits. The fourth mass of the QBCP can be considered as a spacecraft and its motion is described by a Hamiltonian system with three degrees of freedom and depending periodically on time.

We denote the masses of Earth, Moon and Sun, by $1-\mu$, μ and m_s, respectively. To express the equations of the QBCP, we use a synodical system of reference. That is a rotating pulsating frame centered at the Earth–Moon barycenter, in such a way that the Earth and the Moon are located at fixed points $(\mu, 0, 0)$ and $(\mu - 1, 0, 0)$, respectively (see figure 1). In this synodical system, the Sun moves clockwise in a quasi-circular periodic orbit of radius a_s. Its period is denoted by T and the corresponding frequency is ω_s. In this work, the values of the parameters of the QBCP have been set up as

$$\begin{aligned} \mu &= 0.0121505816, \\ a_s &= 388.81114, \\ \omega_s &= 0.925195985520347. \end{aligned}$$

The mass of the Sun is taken as $m_s = (1-\omega_s)^2\, a_s^3 - 1 \simeq 328900.54$, from the third Kepler's law.

The Hamiltonian of the QBCP is

$$H = \frac{1}{2}\alpha_1(p_x^2 + p_y^2 + p_z^2) + \alpha_2(p_x x + p_y y + p_z z) + \alpha_3(p_x y - p_y x) +$$

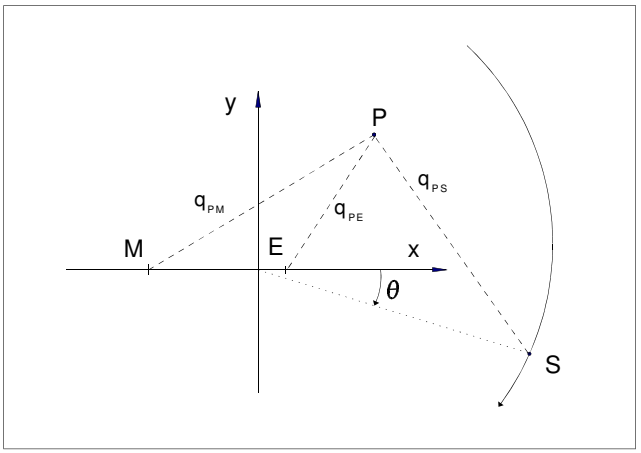

Figure 1. Geometry of the QBCP in a synodical system of reference.

$$+\alpha_4 x + \alpha_5 y - \alpha_6 \left(\frac{1-\mu}{q_{pe}} + \frac{\mu}{q_{pm}} + \frac{m_s}{q_{ps}} \right) , \tag{1}$$

where

$$\begin{aligned} q_{pe}^2 &= (x-\mu)^2 + y^2 + z^2 , \\ q_{pm}^2 &= (x-\mu+1)^2 + y^2 + z^2 , \\ q_{ps}^2 &= (x-\alpha_7)^2 + (y-\alpha_8)^2 + z^2 , \end{aligned}$$

and α_k are known T-periodic functions. For the Earth-Moon-Sun case, the Fourier coefficients of the α_k functions decay quickly, so it is necessary to keep a reduced number of coefficients in order to achieve high accuracy. Moreover, α_1, α_3, α_4, α_6 and α_7 are even functions. The other ones, α_2, α_5 and α_8 are odd. A set of coefficients of the α_k functions can be found in (Andreu, 1998).

In the QBCP, the L_2 point is not an equilibrium point, therefore it is defined geometrically. Around L_2 there are periodic orbits and families of 2D and 3D tori. A full description of the dynamics in a large neighbourhood around L_2 was presented in (Andreu, 2001). This description was performed through the reduction to the center manifold of the Hamiltonian of the QBCP. Besides the center manifold, the dynamics around L_2 is dominated by a highly hyperbolic component. Typically, after a T time span (about 29 days) a small error is amplified by a factor of 10^6.

Unfortunately, the Halo orbits are outside the zone where the dynamics of the reduced Hamiltonian agree with the one of the QBCP. In order to obtain a description of the family of Halo orbits, other

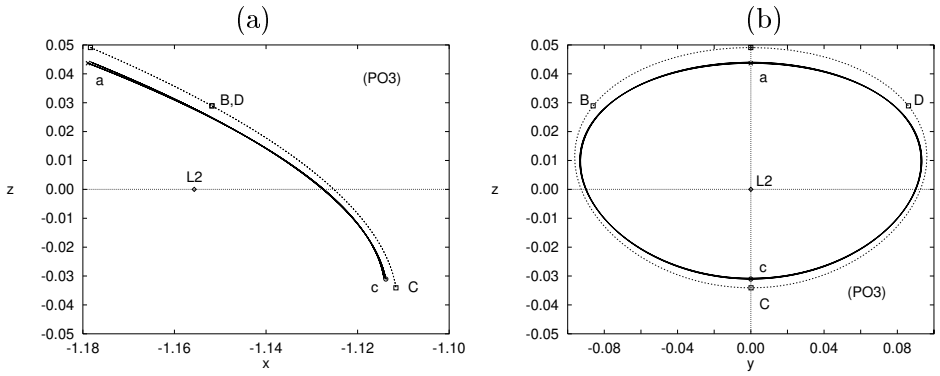

Figure 2. Halo periodic orbits of the QBCP around L_2 in a 1:2 resonance. The dotted line corresponds to a $T/2$-periodic orbit of the RTBP. (a) (x, z) projection of the orbits PO3a,c. (b) (y, z) projection of the previous orbits.

mathematical methods should be used. One of them is a numerical method for the computation of invariant tori, which is going to be shown in the next section.

Concerning periodic orbits, we define a p:q resonance as a pT-periodic orbit revolving q times around L_2. In other words, a p:q resonant periodic orbit has mean motion around L_2 equal to $2q\pi/(pT)$. In the QBCP, most of the $p : q$ resonant orbits are related to periodic orbits of the RTBP with period pT/q.

The main feature of the Halo orbits in the QBCP is the existence of a 1:2 resonance (Andreu, 1998). These periodic orbits are shown in figure 2, labelled here as PO3a,c. Initial points of these orbits for $t = 0$ are marked with $\circ$ or $\times$, depending on their stability character inside the center manifold. The orbit PO3a has a slight hyperbolic part and PO3c the elliptic counterpart. We also want to comment that a $T/2$-periodic Halo orbit of the RTBP is shown as reference in figure 2 with a dotted line.

3. A method for the computation of invariant tori

In this section, a method for the computation of invariant tori is presented. This method is due to À. Jorba (Castellà et al., 2000) (Jorba, 1999). There are some other methods for the computation of invariant tori (see, for example, (Andreu, 1998) and (Simó, 1998)), but presently the Jorba's method is the most efficient one for the problem that we are interested in.

The Jorba's method can be used for the computation of a invariant tori in the general context of a dynamical system as

$$\dot{x} = f(x,t)\ , \qquad x \in \mathbb{R}^n\ , \tag{2}$$

where $f \in C^1$ in a certain domain and T-periodic on t. To simplicity, the method is presented in particular in the case of a 2D torus, but it can be generalised easily to a higher dimensional torus.

The main idea of the Jorba's method is to reduce the problem to the computation of the Fourier coefficients of a section of an invariant torus. Let g be the time T map defined by the flow of (2). The goal is to get an invariant curve $\gamma : \mathbb{S}^1 \to \mathbb{R}^n$ with a given rotation number ρ. That is

$$g(\gamma(\theta)) = \gamma(\theta + 2\pi\rho)\ , \qquad \forall \theta \in [0, 2\pi]\ . \tag{3}$$

The curve γ can be expressed as

$$\gamma(\theta) = a_0 + \sum_{k\geq 1} a_k \cos(k\theta) + b_k \sin(k\theta)\ , \tag{4}$$

where $a_k, b_k \in \mathbb{R}^n$, $\forall k \in \mathbb{N}$. To determine γ with a given precision, it is only necessary to compute the Fourier coefficients for all k less than a certain N. For this purpose, (3) is discretised for $\theta_j = 2\pi j/(2N+1)$, $j = 0, \ldots, 2N$, obtaining $(2N+1)n$ equations, which can be solved numerically by means of Newton's method. In this way, the unknown coefficient a_k, b_k are obtained. We want to point out that the parametrisation of the curve (4) is not unique. To avoid the lack of uniqueness, it is necessary to put an additional condition, which can be, for instance, that one of the components of $\gamma(0)$ has a prefixed value.

Finally, we want to comment that, in the case of highly unstable tori, instead of computing a section of the torus, it is convenient to use several sections $\gamma_0, \ldots, \gamma_{m-1}$. In such case, the Fourier coefficients of the m curves are computed from the invariance equations

$$\left.\begin{aligned} g_i(\gamma_i(\theta)) &= \gamma_{i+1}(\theta)\ , \qquad i = 0, \ldots, m-2, \\ g_{m-1}(\gamma_{m-1}(\theta)) &= \gamma_0(\theta + 2\pi\rho)\ , \end{aligned}\right\} \forall \theta \in [0, 2\pi],$$

where g_i is the map defined by the flow of (2) from time $t = iT/m$ to $t = (i+1)T/m$, for $i = 0, \ldots, m-1$.

4. The Halo family of the QBCP

In the RTBP, it is well-known the dynamics around the equilibrium point L_2, whose linear stability character is of the form center×center× saddle. Around L_2, there are two Lyapunov families of periodic orbits emanating from this equilibrium point. One of these families of periodic orbits lie on the plane of the motion of the primaries (the xy-plane), and it is called the planar family. The planar Lyapunov orbits near the equilibrium point are elliptic-hyperbolic. The hyperbolic directions are on the xy plane, while the elliptic one corresponds to the z coordinate. Following the planar family, increasing the size of the periodic orbits, a bifurcation appears that is associated with a change of stability in the z direction. In that bifurcation, two families of Halo periodic orbits start. The two families are symmetric with respect to the xy-plane. Halo orbits are characterised by the fact that they never cross the primaries axis.

From the bifurcating point, Halo orbits of the RTBP are elliptic-hyperbolic, at least for a wide range of amplitudes. Related to the elliptic part, around each Halo orbit, there is a uniparametric (Cantorian) family of 2D tori (called quasi-halo tori (Gómez et al., 1998)). These tori have two basic frequencies: the inner frequency of the Halo orbit and a frequency close to the normal frequency of the Halo orbit. In fact, the second frequency depends on the amplitude of the quasi-halo orbit with respect to its core Halo orbit and, of course, on the amplitude of the core Halo orbit. Quasi-halo orbits also keep an exclusion zone around the axis of the two primaries.

The QBCP can be considered as a time periodic perturbation of the RTBP. Keeping this in mind, it is easy to understand that L_2 is not an equilibrium point of the QBCP, but there is a small periodic orbit (PO1) around it, which inherit the stability character of the L_2 point of the RTBP. Around PO1, there are two Lyapunov families of 2D tori, emanating from that periodic orbit. These families of 2D tori are not continuous, they are Cantor sets of tori. One of the families of tori starts in the z direction, and the other lies on the xy-plane. The planar family have several changes of stability in the z direction which are related to different branches of 2D resonant tori (Andreu et al., 1999b). One of these changes of stability is associated with the bifurcation where Halo 2D tori are born. In fact, as in the RTBP, there are two families symmetric with respect to the xy plane. These families are not continuous, they are Cantor sets of tori (Jorba et al., 1997).

Halo 2D tori have been computed using the Jorba's method. Since these tori are highly unstable, four sections equally spaced on time were used γ_i, $i = 0, 1, 2, 3$. Each torus has two basic frequencies, its inner

frequency ω_p and the synodic frequency, ω_s. Consider a fixed value of the rotation number ρ. We recall that ρ is defined modulus one. In fact, we have used

$$\rho = \frac{\omega_p}{\omega_s} - 2 \, ,$$

because all the values of the rotation numbers considered in this work are near $2\omega_s$.

To compute invariant tori of the QBCP, it is useful to consider a family of Hamiltonians depending on one parameter:

$$H_\epsilon = H_{RTBP} + \epsilon \, (H_{QBCP} - H_{RTBP}) \, ,$$

for $\epsilon \in [0, 1]$. In this way, a continuation method is used to follow an invariant curve from the RTBP ($\epsilon = 0$) to the QBCP ($\epsilon = 1$). The process of continuation can be applied while no bifurcations occur. As initial invariant curve for $\epsilon = 0$, a periodic orbit with a period of $2\pi/\omega_p$ can be used. We notice that any periodic orbit is an invariant curve for the time T map of the flow of the RTBP.

Several Halo tori of the QBCP were computed with the method just described, using a few steps of a continuation method. From each torus of the QBCP, it is possible to continue the family of tori by varying the rotation number ρ (another continuation method). In spite of the fact that the Halo family is a Cantor set, we want to stress that it is possible to follow the family of tori as if it were a continuous family, except when big gaps appear.

To display the computed families of Halo tori, we choose a representing point of each torus as follows. Consider the intersection of γ_0 with the plane $y = 0$, which typically is a set of two points. The representing point of a torus is the point with maximum z coordinate in the intersection of γ_0 with $y = 0$.

Figures 3a,b shows several branches of the Halo family of 2D tori of the QBCP (solid line) and the family of Halo periodic orbits of the RTBP (dashed line). The point marked with a cross for $\rho = 0$ corresponds to the resonant periodic orbit PO3a. From now on, in all the figures, normalised coordinates have been used. This means that the origin of coordinates is the L_2 point, the unit of length is the L_2-Moon distance (about 60000 Km) and, x and y axis are taken in the opposite direction of section 2.

In figures 3a,b, it is shown that the Halo family of the QBCP has several big gaps in the zone of $\rho < -0.0065$. From now on, this zone is going to be called the R zone. It is believed that these gaps are related to resonances involving the normal frequency of the Halo tori, but this fact has not been checked out yet.

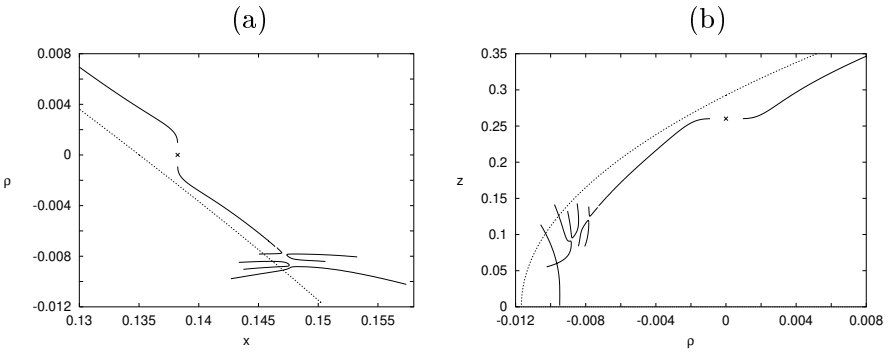

Figure 3. Family of Halo periodic orbits of the RTBP and Halo family of 2D tori of the QBCP. The cross corresponds to the periodic orbit PO3a. (a) (x, ρ) projection. (b) (ρ, z) projection.

Another feature of the Halo family which needs to be commented is the apparent gap around $\rho = 0$. This gap is probably very much smaller than it seems in the figure. The reason of this apparent gap comes from the numerical difficulties in computing invariant tori of the Halo family near the resonance. When Halo family is getting closer to the resonance, sections γ_i tend to the invariant manifolds of the periodic orbit PO3a and so, the number of Fourier coefficients needed for an accurate representation of γ_i increases a lot. The study of the dynamics in the neighbourhood of the 1:2 resonance is now in progress.

5. Translunar Halo orbits of the REMS

The main motivation for introducing the QBCP was the desire of obtaining translunar Halo orbits of the REMS for a long time interval. Several people have been working on this topic before. In (Farquhar et al., 1973), Farquhar and Kamel computed analytical quasi-periodic Halo orbits for a simplified model of the REMS. In (Gómez et al., 1985) G.Gómez *et al.* obtained numerical Halo orbits of the REMS using a parallel shooting method and taking as initial guess Halo orbits of the RTBP and quasi-periodic orbits, computed semi-analytically, of some intermediate simplified model. However, it was difficult to compute this kind of orbits for a time interval longer than 2-3 years. Typically, a Halo orbit in a vicinity of the L_2 libration point of the REMS has a inner period close to two weeks, so many revolutions are required for a prolonged time interval. The first Halo orbits of the REMS for long time span (more than 20 years) were presented in (Andreu et al., 1999a) and (Andreu, 1998).

But, before starting the study of the Halo orbits of the REMS, it is necessary to define rigorously what a Halo orbit of the REMS is. A simple definition could be: a Halo orbit is an orbit revolving, in the configuration space, around a collinear libration point (defined geometrically, of course) never passing through a neighbourhood of the axis joining the two primaries (Earth-Moon, in our case). But, this is a too rough definition. A neighbourhood of the libration point, excluding a neighbourhood of the primaries axis will be denoted as *Halo domain*.

Assuming that the Solar System is quasi-periodic (this is not true, but it is a good approximation for practical purposes during a moderate time span) then Halo orbits are also quasi-periodic, having all the frequencies of the Solar System. Most of them, probably with an amplitude rather small. As we said before, in the RTBP, there are Halo periodic orbits and quasi-halo orbits. This suggests the following definitions. A *Halo orbit of the real Earth-Moon system* is an orbit lying forever in the Halo domain and having, as basic frequencies, the ones of the Solar System and one single inner frequency. In a similar way, *quasi-halo orbits of the real Earth-Moon system* have two inner frequencies, beyond the external ones. One of them plays the role of normal frequency. Both kind of orbits are usually called Halo, but we will be more precise when it is required.

5.1. Methodology

We are interested in looking for an orbit of the REMS, which is a solution of a differential equation as

$$\dot{x} = F(t, x) \ , \tag{5}$$

where $x \in \mathbb{R}^6$ (position and velocity) and the vector field F can be computed from the JPL ephemeris. One of the difficulties to get Halo-like orbits of the REMS for a long time interval is that they are highly unstable. Therefore, to compute numerically Halo orbits, it is convenient to use a parallel shooting method (Stoer et al., 1980). To use the parallel shooting method, it is required to have several points

$$(t_0, \bar{x}_0), (t_1, \bar{x}_1), \ldots, (t_n, \bar{x}_n) \ ,$$

which are taken as a first approximation of the wanted orbit. Those points can be taken on a quasi-periodic Halo orbit of the QBCP. The objective is to refine iteratively the initial points, in order that the different orbits which go through them match together and give (approximately) a single orbit of (5).

Let $\phi(t, t', x)$ be the flow of the equation (5) going from time t to t' with initial condition x. We consider a set of fixed times $\{t_k\}$, for

$k = 0, \ldots, n$, and we want to compute the corresponding states $\{x_k\}$, for $k = 0, \ldots, n$, satisfying the matching equations:

$$\phi(t_k, t_{k+1}, x_k) = x_{k+1} \ , \qquad k = 0, \ldots, n-1 \ . \tag{6}$$

To apply Newton's method to solve these equations, we linearise the system getting

$$\begin{pmatrix} A_1 & -I & & & \\ & A_2 & -I & & \\ & & A_3 & -I & \\ & & & \ddots & \ddots \\ & & & & A_n \quad -I \end{pmatrix} \begin{pmatrix} \Delta x_0 \\ \Delta x_1 \\ \Delta x_2 \\ \vdots \\ \vdots \\ \Delta x_n \end{pmatrix} = \begin{pmatrix} b_1 \\ b_2 \\ b_3 \\ \vdots \\ b_n \end{pmatrix} \ , \tag{7}$$

where A_k are 6×6 matrices coming from the integration of the variational equations of (5); the independent term is formed by the vectors $b_k = x_k - \phi(t_{k-1}, t_k, x_{k-1})$ and the quantities Δx_k are the corrections to the states x_k. We notice that the linear system is infradetermined, having $6n$ equations and $6n + 6$ unknowns.

System (7) can be solved, for instance, adding some minimising condition for the corrections Δx_k. In a system of the form $A\Delta x = b$, requiring to minimise

$$\sum_{k=0}^{n} (\Delta x_k)^2 \ ,$$

leads to $\Delta x = A^T (A\, A^T)^{-1} b$.

For very large linear systems, it is also possible to require only that

$$\sum_{j=0}^{p} (\Delta x_{j \cdot m})^2 \ , \tag{8}$$

is minimum, where $p = n/m$ and m is an integer dividing n. Then, the linear system (7) is reduced to another as

$$\begin{pmatrix} B_1 & -I & & \\ & B_2 & -I & \\ & & \ddots & \ddots \\ & & & B_p \quad -I \end{pmatrix} \begin{pmatrix} \Delta x_0 \\ \Delta x_m \\ \Delta x_{2m} \\ \vdots \\ \Delta x_{pm} \end{pmatrix} = \begin{pmatrix} c_1 \\ c_2 \\ \vdots \\ c_p \end{pmatrix} \ , \tag{9}$$

where

$$\begin{aligned} B_j &= A_{i+m} A_{i+m-1} \cdots A_{i+1} \ , \\ c_j &= A_{i+m}(\cdots (A_{i+3}(A_{i+2}\, b_{i+1} + b_{i+2}) \cdots) + b_{i+m} \ , \end{aligned}$$

for $j = 1, \ldots, p$ and being $i = (j-1)m$. We want to stress that (9) looks like a parallel shooting method using only the set of times $\{t_{jm},\ j = 0, \ldots, p\}$. The main difference is that, to compute the matrices B_j, we do not integrate the variational equations of (5) from t_{jm} to $t_{(j+1)m}$, but we take the composition of the A_{jm+k} matrices using arcs which we hope are closer to the correct solution.

To compute Halo orbits of the REMS, an extra condition can be added to the matching equations (6). Assume that the first point of the orbit $\bar{x}_0$ is on the plane $y = 0$. Then, it is possible to require that the y component of Δx_0 be zero. This condition is related to the fact that the Halo orbits have a free phase.

With the method described above, several quasi-halo orbits of the REMS were computed in (Andreu, 1998), but most of those orbits exhibited large components in the normal frequency. We notice that, generically, the parallel shooting method produces a quasi-halo orbit close (in some sense) to the initial orbit. There is no reason at all to assume that the orbit obtained has only one inner frequency.

However, it has been checked for a wide range of amplitudes that, using a *relaxed* Newton's method, it is possible to obtain Halo orbits of the REMS almost without normal component. Using this relaxed method, the sequence of states, $\{x_k^{(j)}\}_j$, are computed as

$$x_k^{(j+1)} = x_k^{(j)} + r\Delta x_k^{(j)} \ ,$$

where $\Delta x_k^{(j)}$ is obtained from (7) and $r \in (0, 1)$.

5.2. The results

Using the method just described, more than thirty Halo orbits of the REMS have been computed for a time span of 15119 days (about 41 years). Initial points for the parallel shooting method are taken from Halo orbits of the QBCP. The time interval between two consecutives points has been $\Delta t = T/64$, which means about two points per day. The number of points has been chosen $n = 32769$ and the minimising condition (8) has been used with $m = 16$. The relaxed Newton's method has been usually applied with $r = 0.2$. In this way, the convergence is very slow, but, in most cases, the orbit tends to an orbit of the REMS with a normal component rather small. Typically, for each orbit, we have computed 20 iterates of the method with $r = 0.2$, and right after, some few iterates more, without relaxation ($r = 1$).

Figures 4a-d show several projections of a Halo orbit of the QBCP labelled as HOQ1. That orbit was used as initial guess for the Newton's method, obtaining the orbit of the REMS shown in figures 4e-h, which

is labelled as HOR1. Figures 4d,h show the (time, z) projection of orbits HOQ1 and HOR1, respectively. In both cases, the profile formed by the maximum z of each revolution around L_2 shows a long period wave of about 4900 days. From now on, time is measured in days starting from January 1st 2000.

In order to compare an initial orbit of the QBCP with the corresponding final one of the REMS, we take points of each orbit equally spaced on time. In the case of the QBCP, the points for $t = k\,T$, $k \in \mathbb{Z}$ form the curve γ_0 of the Jorba's method of section 3. Figures 5a,b show (x, y) and (y, z) projections of γ_0 of the HOQ1 orbit (dotted line). In the case of the REMS, the corresponding curve can be produced, but this is not a closed curve. Figures 5a,b also show the (x, y) and (y, z) projections of the points of the Halo orbit HOR1 for $t = t_0 + k\,T$, $k \in \mathbb{Z}$, where t_0 is the epoch of the first full moon of year 2000. In the case of the REMS, several small loops are seen. In the next section, we will give the interpretation of these loops.

In section 2, each Halo torus was identified by the point with maximum z coordinate from the intersection of γ_0 with the plane $y = 0$. To compare the family of Halo orbits of the QBCP with the corresponding one of the REMS, a representing point of each torus should be taken in a similar way as in the QBCP. In principle, in the case of the REMS, it might be much more difficult because, in a Halo orbit of the REMS, all the frequencies of the Solar System might appear. Nevertheless, the curve of figure 5 seems to be close to a 2D torus. In this torus, one of the frequencies has an amplitude much bigger than the other one. For this reason, the 2D torus can be approximated by its core which is a closed curve. From this curve, a representing point can be taken in the same way as in the QBCP. The core of the torus has been approximated using a trigonometric polynomial of seventh degree. In this way, the representing point depends on the approximation method, but it has been checked that the differences, by changing the degree of the polynomial, are small enough. Figures 6a,b show (time, x) and (x, y) projections of the section of a Halo orbit of the REMS and its corresponding periodic approximation.

Figures 7a,b show the comparison between Halo families of the QBCP and the REMS, which proves that there is a nice agreement between both families of Halo orbits. We realize that the dominant feature of the Halo family of the REMS comes from the 1:2 resonance, as in the QBCP. However, some discrepancies have been found in the R zone, where some of the computed orbits of the REMS exhibit an important normal component. It seems that the Halo family of the REMS also have some gaps as the one of the QBCP, but these gaps

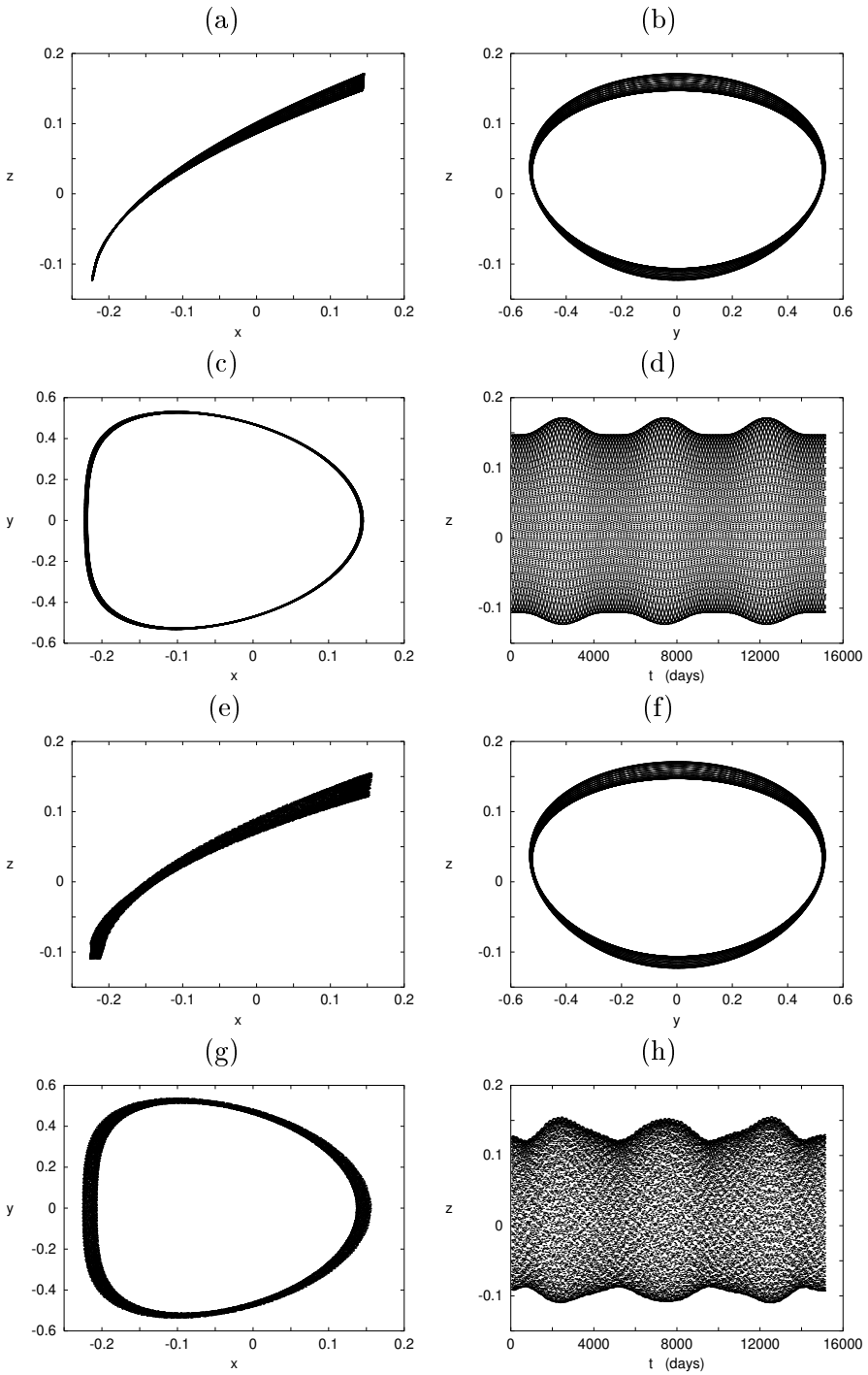

Figure 4. (a)-(d) Halo orbit of the QBCP labelled as HOQ1. (e)-(h) Halo orbit of the REMS labelled as HOR1 and computed from HOQ1.

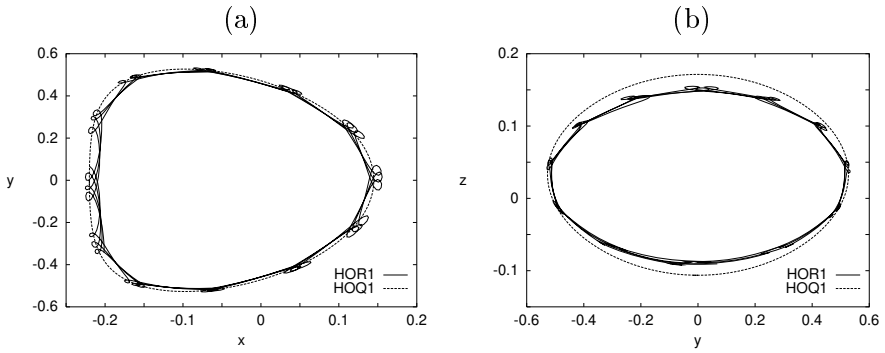

Figure 5. Section for time $t = t_0 + kT$, $k \in \mathbb{Z}$, of the orbits HOQ1 and HOR1. In the case of HOQ1, $t_0 = 0$. For HOR1, t_0 corresponds to the first full moon of year 2000.

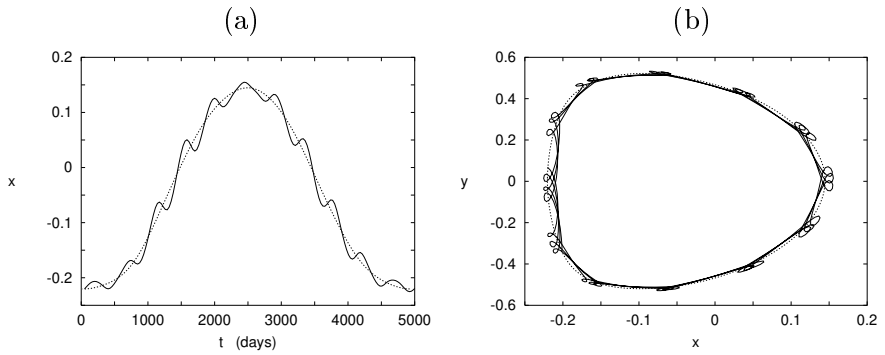

Figure 6. Section for time $t = t_0 + kT$, $k \in \mathbb{Z}$, of the Halo orbit HOR1 of the REMS and periodic approximation of this section (dotted line).

are shifted about 0.001 units in the rotation number, from one model to the other.

5.3. Frequency analysis

The motion of the Moon around the Earth is really quite complicated. As a first approximation, the orbit of the Moon can be considered as an ellipse of eccentricity 0.0549 and semimajor axis of 384 400 km. The plane of the orbit of the Moon is inclined to about 5° with respect to the ecliptic plane. Moreover, the ascending node is moving clockwise with a period of 18.61 years. On the other hand, the perigee of the Moon advances on the plane of the orbit taking 8.85 years for each revolution. The basic frequencies of this motion are given in adimensional units in table I.

As we have said before, it is expected that Halo orbits of the REMS have all the frequencies of the Solar System. Moreover, there is no rea-

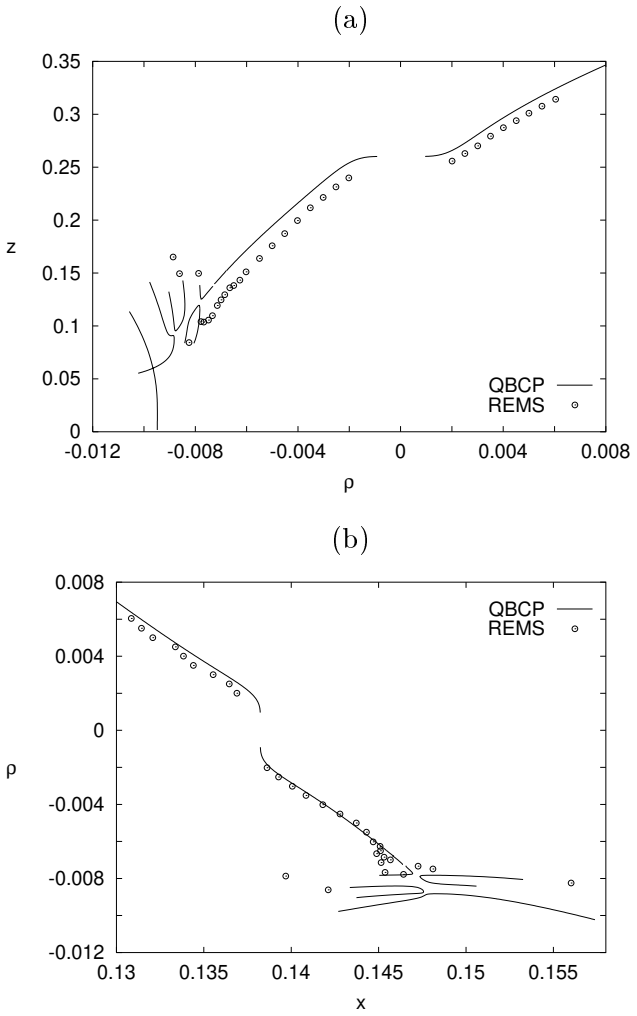

Figure 7. Comparison between Halo families of the QBCP and the REMS. (a) (ρ, z) projection. (b) (x, ρ) projection.

son at all to think that the parallel shooting method is going to obtain a Halo orbit without normal component (sometimes also called "pure" Halo orbit). In fact, generically, this numerical method detects a quasi-halo orbit, so the computed Halo orbits have always some component in the normal frequency.

To study the main frequencies involved in the Halo family, we have performed Fourier analysis of the computed Halo orbits. This analysis of frequencies were done with the software provided by J.M. Mondelo, which uses a slight modification of the Laskar's method to detect relative maxima of the Fourier Transform (Laskar et al., 1992) (Gómez

Table I. Main frequencies of the Moon's orbit and other important related frequencies.

frequency		period	period's name
	1	27.32 days	sidereal month
$\omega_s =$	0.92519599	29.53 days	synodical month
$\omega_{peri} =$	0.00845478	8.85 years	
$\omega_{node} =$	0.00401884	18.61 years	
$\omega_a = 1 - \omega_{peri} =$	0.99154522	27.55 days	anomalistic month
$\omega_d = 1 + \omega_{node} =$	1.00401884	27.21 days	draconitic month
$\omega_b = \omega_{peri} + \omega_{node} =$	0.01247362	6.00 years	

et al., 2001). After the Fourier analysis, it is necessary to identify the obtained frequencies as a linear combination of some frequencies having physical meaning, and it is not an easy task.

As an example of the computations done, we give the tables II, III and IV, corresponding to the orbits labelled as HOQ2, HOR2 and HOR3, respectively. The orbit HOQ2 is a Halo 2D torus of the QBCP, whose rotation number is $\rho = -6.5 \cdot 10^{-3}$. The orbits HOR2 and HOR3 are Halo orbits of REMS and they were computed from HOQ2. In the case of HOR2, 20 iterates of the relaxed Newton's method with r=0.2 were used, followed by 6 extra iterates without relaxation. In the case of HOR3, only the two initial iterates were relaxed and after that, 12 iterates without relaxation were computed.

Tables II, III and IV show the thirty frequencies with largest amplitudes coming from the analysis of the z component of the orbits HOQ2, HOR2 and HOR3, respectively.

In table II, we see that all the frequencies produced by the Fourier analysis can be interpreted, of course, as a linear combination of the inner frequency of the orbit, ω_p, and the synodic frequency, ω_s. The last column of table II shows the corresponding amplitude $C_j = \sqrt{A_j^2 + B_j^2}$, where B_j and A_j are the amplitudes in sine and cosine terms, respectively. Here, the C_j amplitudes are shown as an indicator of the relative importance of each frequency.

Table III shows an interpretation of the frequencies of the orbit HOR2. All the frequencies have been identified as a linear combination of the inner frequency ω_p, the normal frequency ω_n and $\tilde{\omega}_k$, $k \in \{s, a, b, c\}$, where $\tilde{\omega}_k$ is close to ω_k. We realize that the orbit HOR2 has a small normal component because the first frequency related to the normal one is the 20th frequency of the table. Apart from the inner

frequency of the orbit, the second frequency that is important is $2\omega_s$. This frequency appears for a wide range of Halo orbits because of the proximity of the 1:2 resonance. The other frequencies used in table III as basic frequencies are $\tilde{\omega}_a$, $\tilde{\omega}_b$ and $\tilde{\omega}_c$. It is seen that there are a lot of frequencies of this table related to the anomalistic frequency ω_a. The loops seen in figure 5 are produced by the frequencies associated with ω_a. The frequency ω_b is the difference between the anomalistic and the draconitic frequencies, and its corresponding period is about 1/3 of the Saros period.

Table IV shows an interpretation of the main frequencies of the orbit HOR3. In this case, the normal component is much more important. The frequencies not related to the normal one can be compared with the corresponding frequencies of the previous table and a nice agreement is found. Nevertheless, among the thirty frequencies of table IV, there is no frequency directly related to ω_c.

Figures 8a-c show the graph of the analysed functions $z(t)$ of the previous orbits. We recall that those orbits have an inner period of about fifteen days. So figures 8a-c show more than one thousand oscillations of z. However, in these figures, what is certainly very significant is the profile formed by the relative maxima and minima of z. In figure 8a the maxima show a long period wave. Its period is $2\pi/(\omega_p - 2\omega_s)$, about 4500 days. The profile of figures 8b,c also show a similar wave. In the case of figure 8c, there is another superimposed wave related to the normal component of the orbit. Its period is $2\pi/\omega_n$, about 820 days. The long period wave is generated mainly by the term with frequency $2\omega_s$. The shorter period wave is produced mainly by the terms with frequencies $\omega_p \pm \omega_n$.

6. Conclusion and outlook

In this paper, we have summarised all the tools necessary to compute systematically Halo orbits of the REMS, which are

1. The equations of the QBCP, a model of reference for the motion of a spacecraft in the Earth-Moon-Sun system.

2. A method for the computation of invariant tori, which is used to compute Halo orbits of the QBCP.

3. The parallel shooting method with a certain minimising condition and a relaxed Newton's method are used to obtain Halo orbits of the REMS from Halo orbits of the QBCP.

Table II. Identification of thirty frequencies with the largest amplitudes of the z component of the orbit HOQ2. These frequencies can be expressed as a linear combination of $\omega_p = 1.84437820$, $\tilde{\omega}_s = 0.92519599$. Moreover, $d_j = \omega_j - |k_p\omega_p + k_s\tilde{\omega}_s|$ and C_j is the total amplitude.

ω_j	k_p	k_s	d_j	C_j
1.84437819	1	0	−1.360e−08	1.229e−01
1.85039195	0	2	−3.140e−08	1.036e−02
3.68875638	2	0	−1.840e−08	9.232e−03
1.85640574	1	−4	−1.700e−08	1.952e−03
0.00601402	1	−2	2.450e−07	1.810e−03
5.53313456	3	0	−3.530e−08	1.610e−03
0.01202759	2	−4	3.138e−08	5.866e−04
1.83235061	3	−4	−3.390e−08	4.828e−04
3.68274287	3	−2	2.459e−07	3.818e−04
3.69476979	1	2	−3.851e−07	3.525e−04
7.37751275	4	0	−4.630e−08	3.276e−04
1.82633691	4	−6	5.340e−08	2.014e−04
3.70078392	0	4	−4.110e−08	1.806e−04
5.53914807	2	2	−3.135e−07	1.577e−04
5.52712079	4	−2	−2.670e−08	1.379e−04
0.01804133	3	−6	−1.451e−08	7.957e−05
9.22189094	5	0	−5.770e−08	7.580e−05
1.86241954	2	−6	4.800e−09	6.775e−05
2.76957418	1	1	−1.080e−08	5.946e−05
5.54516210	1	4	−5.510e−08	5.504e−05
0.91918224	1	−1	2.953e−08	5.111e−05
7.37149927	5	−2	2.494e−07	4.240e−05
7.38352619	3	2	−3.863e−07	3.904e−05
1.83836316	2	−2	−1.264e−06	3.678e−05
11.06626913	6	0	−6.800e−08	1.863e−05
7.38954029	2	4	−6.700e−08	1.376e−05
9.21587743	6	−2	2.101e−07	1.322e−05
3.67071504	5	−6	−2.020e−08	1.094e−05
9.22790435	4	2	−4.324e−07	1.082e−05
1.81430918	6	−10	−1.185e−07	9.341e−06

Table III. Identification of thirty frequencies with the largest amplitudes of the z component of the orbit HOR2. These frequencies can be expressed as a linear combination of $\omega_p = 1.84437553$, $\tilde{\omega}_s = 0.92520874$, $\tilde{\omega}_a = 0.99154504$, $\tilde{\omega}_b = 0.01235896$, $\omega_c = 0.00393221 \simeq \omega_{node}$, $\omega_n = 0.03304531$. Moreover, $d_j = \omega_j - |\sum_i k_i \omega_i|$ and C_j is the total amplitude.

ω_j	k_p	k_s	k_a	k_b	k_c	k_n	d_j	C_j
1.84437553	1	0	0	0	0	0	−9.000e−10	1.029e−01
1.85041749	0	2	0	0	0	0	6.000e−09	1.040e−02
2.83592057	1	0	1	0	0	0	2.500e−09	8.999e−03
0.85283070	1	0	−1	0	0	0	2.098e−07	7.965e−03
3.68875097	2	0	0	0	0	0	−8.790e−08	7.499e−03
1.85673449	1	0	0	1	0	0	−5.000e−09	3.056e−03
0.00603978	1	−2	0	0	0	0	−2.166e−06	2.408e−03
1.83838605	2	−2	0	0	0	0	5.247e−05	1.976e−03
2.70322430	1	2	−1	0	0	0	−2.367e−05	1.937e−03
0.98553005	1	−2	1	0	0	0	2.696e−05	1.649e−03
4.68029623	2	0	1	0	0	0	1.321e−07	1.344e−03
5.53312625	3	0	0	0	0	0	−3.401e−07	1.261e−03
0.99154697	0	0	1	0	0	0	1.934e−06	1.209e−03
1.83202306	1	0	0	−1	0	0	6.489e−06	1.000e−03
2.69720954	2	0	−1	0	0	0	3.516e−06	9.521e−04
0.01234734	0	0	0	−1	0	0	−1.162e−05	9.244e−04
2.84195790	0	2	1	0	0	0	−4.615e−06	9.180e−04
3.82746537	1	0	2	0	0	0	−2.387e−07	6.857e−04
1.85828192	0	2	0	0	2	0	1.570e−08	6.098e−04
1.81137336	1	0	0	0	0	−1	4.314e−05	5.826e−04
0.85888428	0	2	−1	0	0	0	1.184e−05	5.674e−04
1.82591224	2	−2	0	−1	0	0	−6.238e−05	5.094e−04
1.87746398	1	0	0	0	0	1	4.314e−05	3.988e−04
2.82991727	2	−2	1	0	0	0	3.865e−05	3.832e−04
1.84652822	0	2	0	0	−1	0	4.295e−05	3.475e−04
6.52467171	3	0	1	0	0	0	7.530e−08	3.466e−04
4.54760323	2	2	−1	0	0	0	−2.027e−05	3.119e−04
1.81902583	1	0	0	−3	3	0	−6.945e−05	2.998e−04
3.70117806	2	0	0	1	0	0	6.804e−05	2.989e−04
1.91915419	1	−1	1	1	−1	0	1.562e−05	2.756e−04

Table IV. Identification of thirty frequencies with the largest amplitudes of the z component of the orbit HOR3. These frequencies can be expressed as a linear combination of $\omega_p = 1.84437858$, $\tilde{\omega}_s = 0.92520370$, $\tilde{\omega}_a = 0.99154498$, $\tilde{\omega}_b = 0.01240083$, $\omega_n = 0.03341382$. Moreover, $d_j = \omega_j - |\sum_i k_i \omega_i|$ and C_j is the total amplitude.

ω_j	k_p	k_s	k_a	k_b	k_n	d_j	C_j
1.84437858	1	0	0	0	0	−3.700e−09	1.033e−01
1.85040739	0	2	0	0	0	−6.100e−09	1.044e−02
2.83592355	1	0	1	0	0	−5.600e−09	9.031e−03
0.85283376	1	0	−1	0	0	1.626e−07	8.007e−03
3.68875701	2	0	0	0	0	−1.459e−07	7.529e−03
1.81096476	1	0	0	0	−1	−1.900e−09	4.488e−03
1.85677941	1	0	0	1	0	−4.900e−09	3.096e−03
1.87779567	1	0	0	0	1	3.268e−06	2.716e−03
0.00602565	1	−2	0	0	0	−3.166e−06	2.405e−03
2.70322632	1	2	−1	0	0	−1.468e−05	1.944e−03
1.83839726	2	−2	0	0	0	4.750e−05	1.932e−03
0.98553246	1	−2	1	0	0	1.630e−05	1.656e−03
0.03341663	0	0	0	0	1	2.806e−06	1.634e−03
1.81694740	0	2	0	0	−1	−4.618e−05	1.600e−03
1.80495734	2	−2	0	0	−1	2.140e−05	1.453e−03
1.87178500	2	−2	0	0	1	2.142e−05	1.414e−03
4.68030213	2	0	1	0	0	−5.800e−09	1.350e−03
5.53313541	3	0	0	0	0	−3.285e−07	1.266e−03
0.99154841	0	0	1	0	0	3.425e−06	1.213e−03
1.88380609	0	2	0	0	1	−1.513e−05	1.111e−03
1.83194391	1	0	0	−1	0	−3.384e−05	1.053e−03
2.69721600	2	0	−1	0	0	3.820e−06	9.546e−04
0.01241305	0	0	0	1	0	1.222e−05	9.509e−04
2.84194936	0	2	1	0	0	−3.017e−06	9.214e−04
0.02741645	1	−2	0	0	1	3.145e−05	7.280e−04
3.82746828	1	0	2	0	0	−2.621e−07	6.882e−04
0.85886884	0	2	−1	0	0	6.417e−06	5.696e−04
0.03941770	1	−2	0	0	−1	−2.494e−05	5.625e−04
1.82568549	0	2	0	−2	0	7.975e−05	5.527e−04
1.86499558	1	−1	1	−1	−1	9.037e−05	4.319e−04

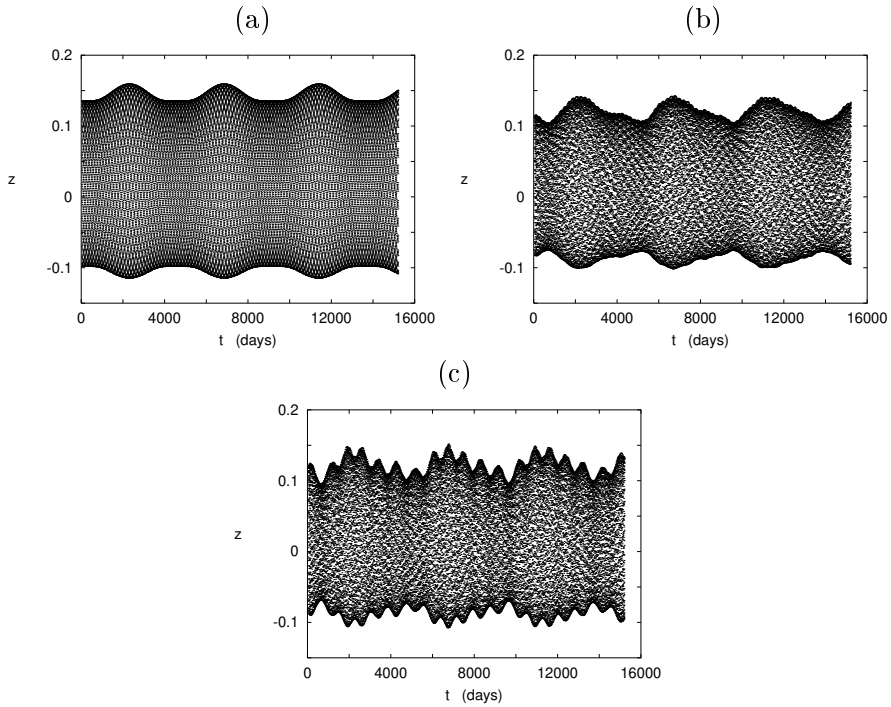

Figure 8. Graph of $z(t)$ of the orbits: (a) HOQ2, (b) HOR2 and (c) HOR3. The profile formed by the relative maxima and minima are very significant.

Presently, we are working on the design of a semianalytical method for the computation of Halo orbits of the REMS. It is expected that this method would allow to use a continuation technique along the Halo family and then a full description of the Halo family would be given.

We want to end this article by expressing our hope that the QBCP will become a model of reference for the design of many future space missions in the Earth-Moon system.

7. Acknowledgements

I would like to express my gratitude to all the people who have contributed in many different ways in the realization of this work. Firstly, I want to thank all the authors of the reports (Gómez et al., 1985), (Gómez et al., 1987), (Gómez et al., 1991) and (Gómez et al., 1993) for allowing me to use all their software and papers. I want to make a special mention of C. Simó and G. Gómez for the valuable knowledge obtained from them. I am also in debt with J.M. Mondelo, for his help in the frequency analysis task. I also want to make reference to

E. Castellà and À. Jorba for their explanations about the method of computation of invariant tori. As a gratitude, my thanks to S.L. Buxton for suggesting some orthographical corrections. This work has been partially supported by the catalan grants CIRIT 1998SGR-00042 and 2000SGR-00027.

References

Andreu, M.A.: 1998, *The Quasi-bicircular Problem*, Thesis, Dept. Matemàtica Aplicada i Anàlisi, Universitat de Barcelona.

Andreu, M.A. : 2001, *Dynamics in the center manifold around* L_2 *in the Quasi-bicircular Problem*, Celestial Mech. (to appear).

Andreu ,M.A. and Simó, C.: 1999a, 'Translunar Halo orbits in the Quasi-bicircular Problem', B.A. Steves and A.E. Roy editors, *The Dynamics of Small Bodies in the Solar System*, NATO ASI (1997, Maratea, Italy), pp. 309–314.

Andreu, M.A. and Simó, C.: 1999b, *Estudio de la estabilidad de una familia de toros 2D del problema Cuasibicircular*, XVI CEDYA/VI CMA, (1999, Las Palmas de Gran Canaria, Spain), Vol. I, pp. 131–138.

Belbruno, E.A. and Miller, J.K.: 1993, *Sun perturbed Earth to Moon transfers with ballistic capture*, Journal of Guidance, Control and Dynamics **16**, 770–775.

Castellà., E. and Jorba, À.: 2000, *On the vertical families of two-dimensional tori near the triangular points of the Bicircular problem*, Celestial Mech. **76**(1), 35–54.

Farquhar, R.W.: 1970, *The Control and Use of Libration-Point Satellites*, NASA TR R346.

Farquhar, R.W, Kamel, A.A.: 1973, *Quasi-periodic orbits about the translunar libration point*, Celestial Mech. **7**, 458–473.

Gabern, F., Jorba, À: 2001, *A restricted four-body model for the dynamics near the Lagrangian points of the Sun-Jupiter system*, Discrete and Continuous Dynamical Systems, series B, V. 1 n. 2, 143-182.

Gómez G., Howell, K.C., Masdemont J. and Simó C.: 1998, *Station-Keeping Strategies for Translunar Libration Point Orbits*, Advances in the Astronautical Sciences 99, 949–967.

Gómez G., Jorba À., Masdemont J. and Simó C.: 1991, *Study refinement of semianalytical halo orbit theory*, ESOC contract 8625/89/D/MD(SC), Final Report.

Gómez G., Jorba À., Masdemont J. and Simó C.: 1993, *Study of Poincaré maps for orbits near Lagrangian points*, ESOC contract 9711/91/D/IM(SC), Final Report.

Gómez G., Jorba À., Masdemont J. and Simó C.: 1993, *Study of the Transfer from the Earth to a Halo orbit around the equilibrium point* L_1, Celestial Mechanics **56**, 541–562.

Gómez G., Koon W.S., Lo, M.W., Marsden, J.E., Masdemont J., Ross, S.D.: 2001, *Invariant Manifolds, the Spatial Three-Body Problem and Space Mission Design*, Astrodynamics Specialist Meeting Quebec City, Canada, AAS01-31.

Gómez G., Llibre J., Martínez R. and Simó C.: 1985, *Station keeping of libration point orbits*, ESOC contract 5648/83/D/JS(SC), Final Report.

Gómez G., Llibre J., Martínez R. and Simó C.: 1987, *Study on orbits near the triangular libration points in the perturbed restricted three body problem*, ESOC contract 6139/84/D/JS(SC), Final Report.

Gómez G., Masdemont J. and Simó C.: 1998, *Quasihalo orbits associated with libration points*, J. of the Astronautical Sci., **46**.

Gómez G., Masdemont J.: 2000, *Some Zero Cost Transfers between Libration Point Orbits*, AAS Paper 00-177, AAS/AIAA Astrodynamics Specialist Conference, Florida.

Gómez, G., Mondelo, J.M. and Simó, C.: 2001 *Refined Fourier analysis: procedures, error estimates and applications*, preprint.

Gómez, G., Lo, M., Masdemont, J. and Museth, K.: 2001, *Simulation of Formation Flight Near Lagrange Points for the TPF Mission*, AAS 01-305.

Gutzwiller, M.C.: 1998, *Moon-Earth-Sun: The oldest three-body problem*, Reviews of Modern Physics, Vol. 70, N. 2.

Huang, S.S.: 1960 *Very restricted four body problem*, NASA Technical Note D-501.

Jorba À.: 1999, *On practical stability regions for the motion of a small particle close to the equilateral points of the real Earth-Moon system*, (preprint).

Jorba À., Masdemont, J.: 1999, *Dynamics in the Center Manifold of the Restricted Three Body Problem*, Physica D, vol. 132, 189–213.

Jorba, À., Villanueva, J.: 1997, *On the persistence of lower dimensional invariant tori under quasi-periodic perturbations*, Journal of Nonlinear Science, **7**, 427–473.

Koon W.S., Lo, M.W., Marsden, J.E., Ross, S.D.: 1999, *The Genesis Trajectory and Heteroclinic Connections*, AAS/AIAA Astrodynamics Specialist Conference, Girdwood, Alaska, AAS99-451.

Koon W.S., Lo, M.W., Marsden, J.E., Ross, S.D.: 2000, *Heteroclinic Connections between Periodic Orbits and Resonance Transitions in Celestial Mechanics*, Chaos V.10, 2, June, 427–469.

Koon W.S., Lo, M.W., Marsden, J.E., Ross, S.D.: 2001, *Low Energy Transfer to the Moon*, Celestial Mechanics and Dynamical Astronomy, (to appear).

Laskar, J., Froeschlé, C., Celletti, A.: 1992, *The measure of chaos by the numerical analysis of the fundamental frequencies. Application to the standard mapping*, Physica D, **56**, 253–269.

Simó, C.: 1998, *Effective Computations in Celestial Mechanics and Astrodynamics*, Modern Methods of Analytical Mechanics and their Applications, Ed. V. Rumyantsev and A. Karapetyan, CISM Courses and Lectures **387**, Springer.

Stoer, J., Bulirsch, R.: 1980, *Introduction to numerical analysis*, Springer-Verlag.

Szebehely, V.: 1967, *Theory of orbits*, Academic Press.

Wiesel, W.: 1984, *The restricted Earth-Sun-Moon problem I: Dynamics and libration point orbits*, Dept. Aeron. and Astron., Air Force Institute of Technology Wright-Patterson AFB, Ohio.